

Interface-dominated magnetical behavior in advanced metal matrix composites

Pili kumari Sahoo, Subhakanta Nayak

College of Engineering Bhubaneswar, BPUT, Odisha, India

Abstract

To obtain particular properties, metal matrix composites, or MMCs, combine a functional or reinforcing secondary phase into a metal matrix. The reinforcement/matrix interface's structure and properties are among the key factors that can influence how mechanically MMCs behave. With a focus on the application of micro- and nano-mechanical testing techniques, this article examines recent advancements in the measurement of the interfacial properties in advanced MMCs. It is demonstrated that researchers can now obtain some of the critical interfacial properties and the effects of reinforcement/matrix interfaces on the deformation and failure mechanisms of the composites that were previously unattainable by conventional methods thanks to the novel in situ and ex situ experimental capability. Furthermore, it is possible to conduct basic and applied research on the mechanical performance of the composites under service conditions thanks to the micro- and nano-mechanical testing platform, which is thought to be a promising and developing field of study.

Introduction

In order to achieve particular mechanical and/or functional properties not possible in the individual constituents and/or metal alloys, metal matrix composites, or MMCs, are composites that incorporate hard reinforcement—typically ceramic—into a metal matrix. For instance, traditional strengthening techniques like precipitate and solid-solution strengthening can greatly boost a metal or alloy's strength, but they have little effect on modulus, which is a direct indicator of the metal's chemical bonding stiffness. However, in MMCs, the load-bearing capacity of the reinforcing phase upon mechanical loading effectively improves the modulus. The reinforcement/matrix interface's structure and properties are among the key factors that could influence the mechanical behavior of MMCs. For instance, the operating failure mechanism of long-fiber reinforced MMCs, also known as "continuously reinforced MMC," is dictated by the strength of the reinforcement/matrix interfacial in relation to the fiber and matrix strengths [1]. The shear-lag model [7,9–11] is frequently used

to estimate the strengthening contribution from the reinforcement in the case of discontinuously reinforced composites, such as those reinforced by particles [2–7] and/or short fibers [8]. In these cases, the load is transferred from the matrix to the reinforcement by shear stresses at their interfaces. As a result, the reinforcement/matrix interface's shear strength becomes crucial.

Although the experimental methodology for determining interfacial properties between dissimilar materials has been well established for macroscopic materials and/or parts [for example, the ASTM standards of A944-99 “Standard Test Method for Comparing Bond Strength of Steel Reinforcing Bars to Concrete Using Beam-End Specimens” and A981-97 “Standard Test Method for Evaluating Bond Strength for 15.2 mm (0.6 in.) Diameter Prestressing Steel Strand, Grade 270, Uncoated, Used in Prestressed Ground Anchors”], direct assessment of the interfacial shear strength of MMCs with micro-/nano-scale reinforcements is sought, but rarely obtained, as a result of the difficulty in its experimental measurement. Rather, the standard approach is to obtain the interfacial strength indirectly through model fitting to macroscopic mechanical data, presuming

specifics about the size, shape, and distribution of the reinforcement.

Over the past 20 years, advances in micro- and nano-mechanical characterization of small-scale specimens have made it possible to examine material properties that were previously unreachable through conventional experimental techniques, resulting in the development of potent new tools [13–15]. The micro-/nano-scale test specimens used in these investigations are created using lithography-based techniques [19] or focused ion beam (FIB) [16–18], after which they undergo compression or uniaxial tension testing using a grip/indenter tip that is specially made for them. These innovative methods enable the direct assessment of interfacial qualities in MMCs with discontinuous reinforcement. This piece emphasizes and examines the significant research advancements made recently in the study of the Interfacial characteristics and mechanical behavior dominated by the interface in sophisticated MMCs. There are two case studies covered in this article: 1) isolating and characterizing a single composite interface within a single test specimen, as well as assessing the combined impact of multiple interfaces within a micro-/nano-sample. The modification of strengthening and

deformation mechanisms connected to the interface is given particular attention. In conclusion, viewpoints and obstacles are highlighted and suggested for additional development in this area.

2. Determination of properties of a single interface

It is now possible to isolate a single interface (or boundary) so that its structure and properties can be identified, thanks to the site-specific fabrication capability of FIB systems. Ng and Ngan [20] and Kunz et al. [21], for instance, created aluminum (Al) micro-pillars with a single grain boundary. It was discovered that the grain boundary effectively lowers the magnitudes and frequencies of the discrete strain bursts by limiting dislocations, preventing them from escaping at the specimen free surface (Fig. 1a [20]). But depending on the precise kind and nature of the boundary, such micro-pillar analysis also shows that the grain boundaries may potentially act as sources of dislocation [21]. Aitken et al. [22] followed this line of work and further carried out in situ compression testing of aluminum bicrystals (Fig. 1b) in a scanning electron microscope (SEM), which revealed frictional sliding along the boundary plane. Specifically, the in situ test captured the

detailed and complete deformation procedure and mechanism during uniaxial compressive loading (Fig. 1c): an initial peak of 156 MPa was reached after the elastic regime, which corresponds to approximately 58 MPa resolved onto the grain boundary plane and slip direction, being 39% less than the critical resolved shear stress for bi-crystalline aluminum nano-pillars with a vertically oriented grain boundary [21]. This initial peak was followed by a sudden softening to about 100 MPa at ~2.5% strain, correlated with the grain boundary sliding event (Fig. 1d). The stress then varied continuously between 79 MPa and 112 MPa for the remainder of the compression test, all the way up to the unloading strain of approximately 16.2%.

Despite the success in studying the deformation mechanisms of interface-containing systems such as polycrystalline materials [19,23,24] and metallic nanolaminates [16–18], where the interface is formed between similar materials (i.e., between two grains of the same materials but with different crystallographic orientations) or between two metal-metal thin films, studying the properties of interfaces formed between two dissimilar materials, such as the metal/ceramic interface, in atypical MMC using micro-

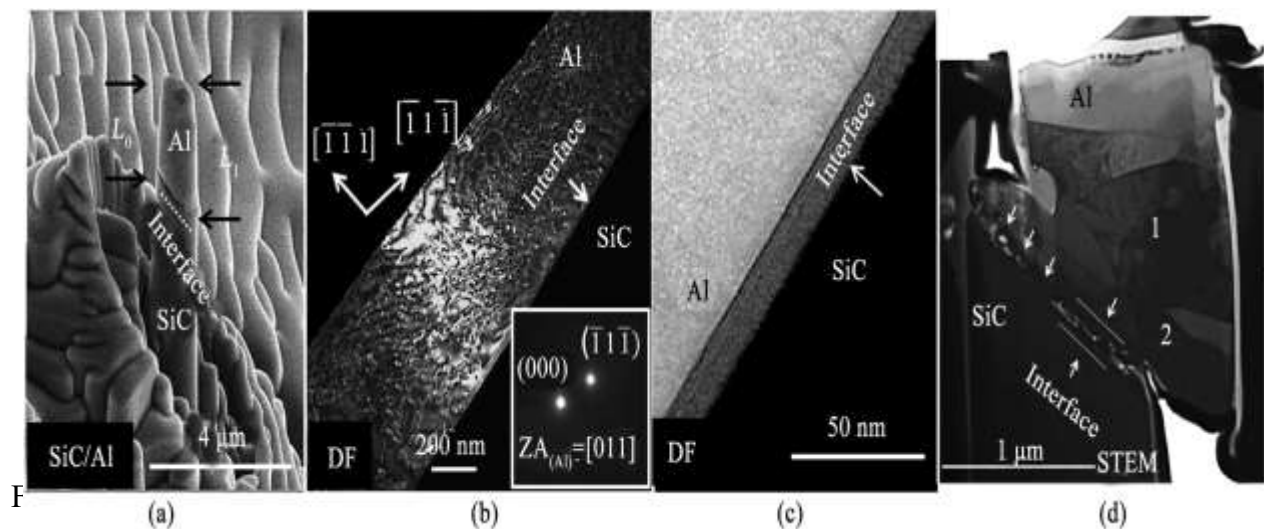
/nano-mechanical characterization, is much more difficult. This difficulty stems from the contrasting properties of the two constituent phases, which would make the fabrication and testing of such interfaces more challenging. Recently, Singh et al. [25] and Lotfian et al. [26] fabricated and tested polycrystalline aluminum/amorphous SiC micro-pillars from sputter-deposited multilayered composite thin films. However, the sputtered composite films have microstructures distinctly different from those of bulk aluminum matrix composites reinforced by SiC particles (SiCp), thus their results may have limited implications for the deformation and failure mechanisms of engineering MMCs. To determine the interfacial failure mechanism of reinforcement/matrix in real discontinuously reinforced MMCs and to estimate the shear strength of their interfaces, Guo et al. [27] fabricated SiC–Al composite micro-pillars containing a 45° slanted interface delivering the maximum resolved shear stress upon uniaxial compressive loading.

SiCp–Al composite is one of the most widely used MMCs in the industry for structural thermal management applications due to its high specific stiffness and

strength, good thermal conductivity, and light weight. Fig. 2a demonstrates a representative as-fabricated ~1 μm-diameter SiC–Al composite micro-pillar. Transmission electron microscopic (TEM) analysis revealed that the grain size in the aluminum layer is on the order of several microns (Fig. 2b), thus the aluminum part of the pillar is essentially single crystalline. The SiC/Al interfacial structure can be tailored by various surface treatments of the SiC reinforcement, e.g., oxidation or hydrofluoric (HF) acid treatment (Fig. 2c). A uniaxial compression test caused shear at the SiC/Al interface (Fig. 2d), and the interfacial shear strength was estimated to be 133 ± 26 MPa, which falls into the same range as shear strengths predicted from theoretical studies [27–29]. The most striking change observed in the post-deformation TEM analysis (Fig. 2d) is the clear grain fragmentation, where the deformed aluminum part contains multiple grains, with grain sizes generally in the range of a few hundreds of nanometers. Such a grain refinement has never been observed in previous studies of single crystalline [30] or bi-crystalline [21,22] aluminum pillars. As the only difference between these studies and the work by Guo et al. [27] is the introduction of the heterogeneous,

inclined SiC/Al interface, this may indicate that the slanted interface confers significant strain gradient during deformation and that the SiC/Al interface serves as an effective barrier for dislocation motion. Guo et al. [27] further argued that the presence of the interface in the pillar prevents dislocation avalanches [31], thereby leading to a

smoother deformation. The isolation and engineering of a single reinforcement/matrix interface in a single micro-/nano-scale specimen may provide insight into the deformation mechanism of discontinuously reinforced MMCs, thus enabling improvements in the design and modeling of advanced MMCs.



characterized by a shorter (L_0) and a longer (L_1) sides. (b) Dark field TEM image of a typical as-fabricated SiC–Al bi-layer lamella structure taken under two beam conditions. (c) A magnified rendition of the interfacial structure under TEM. (d) Post-deformation TEM image of the composite micro-pillar [27] (reprinted with permission from Ref. [27]).

3. Study on the effects of aggregated interfaces

It is now possible to isolate a single interface (or boundary) so that its structure and properties can be identified, thanks to the site-specific fabrication capability of FIB systems. Ng and Ngan [20] and Kunz et al. [21], for instance, created aluminum (Al) micro-pillars with a single grain boundary. It was discovered that the grain boundary effectively lowers the magnitudes and frequencies of the discrete strain bursts by limiting dislocations, preventing them from escaping at the specimen free surface (Fig.

1a [20]). But depending on the pIEvery time a new MMC is developed, more sophisticated reinforcements are always being searched for, found, and then used. A great deal of research has been focused on the creation and characterization of nanocarbon-reinforced MMCs over the last ten years due to the emergence of nanocarbonic materials like carbon nanotubes (CNTs), graphene, and their derivatives [32–34]. These materials have been reported to exhibit exceptionally high strengths (130 GPa) and high Young's modulus values (1 TPa) in their pristine, single-crystalline form [35]. Additionally, their intrinsic properties may still outperform those of conventional fiber and particle reinforcements [8,16] even in the presence of a certain concentration of crystalline defects. Furthermore, the property enhancement conferred by the nanocarbonic reinforcements can well exceed that predicted by the “rule-of-mixtures”, due to the confinement of the dislocations imposed by the interface between the metal and the nanocarbon phases [36–38]. The strengthening and deformation mechanisms of nanocarbonreinforced MMCs are usually very complex due to the simultaneous presence of multiple potential

mechanisms. Kim et al. [36] fabricated graphene/Cu and graphene/Ni nanolaminated composite multi-layers by alternately evaporating metal thin films and transferring monolayer or bilayer graphene onto the metal-deposited substrate, as schematically illustrated in Fig. 3a. As it is difficult to carry out macroscopic mechanical tests on these composite thin films, a uniaxial compression test was conducted on nano-pillars fabricated from the composite films. It was found that the nanolayered composite pillars have extremely highstrengths, achieving more than 30%–50% of the theoretical strength ofthe respective metals, which can be attributed to the obstruction of dislocationsby the graphene layers (Fig. 3b). This reveals the effect ofgraphene (or, in general, other nanocarbon-based reinforcements) on thedeformation mechanism of the matrix metal; however, the fabricationroute is of low throughput, so that the as-fabricated composites are only applicable to thin-film-typed applications, such as flexible electronicsand micro-electro-mechanical systems (MEMS). The process of powder metallurgy (usually described as ball-milling) is characterized by its high strain rate and would result in severe plastic deformation in the milled materials.

Powder metallurgy is an important approach for the fabrication of non-equilibrium alloys and nanocrystalline metals [39,40]. In the past decade, numerous studies have reported the attainment of uniformly distributed CNTs and graphene nanosheets inside a metal matrix through the use of ball-milling processes. The advantages of ball-milling include its simplicity, high efficiency and general applicability. However, the high energy nature of the process and the severe deformation caused by milling may give rise to the fracture and damage of nanocarbon as well as introduce various defects therein. The formation of brittle intermetallic phases may also occur owing to the chemical reaction at the nanocarbon/metal interfaces during ball-milling. Thus, it has been considered that the simple co-milling of CNTs/graphene and metal powders does not well demonstrate the potential of the property enhancement of nanocarbon-reinforced MMCs[16,32].

To minimize the damage caused by high energy ball-milling, Li et al.[16,41] developed a processing methodology in which, instead of co-milling nanocarbon and metal powders together, only the spherical

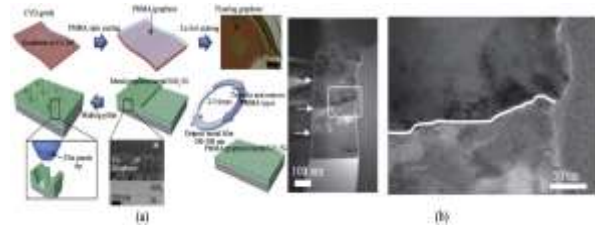


Fig. 3. (a) Fabrication and mechanical characterization of graphene-Cu composites. (b) Obstruction of dislocations at a graphene/Cu interface in a deformed composite nano-pillar [36] (reprinted with permission from Ref. [36]).

metal powders were subjected to the milling procedure. The initially spherical metal powders were then converted into platelets having thicknesses varying from hundreds of nanometers to microns, and CNTs and graphene were absorbed on the platelet surfaces in an organic solvent.

Bulk composite samples suitable for macroscopic tensile tests were subsequently obtained by the drying and sintering of the composite powders and the final deformation processing [16,41]. As high energy milling was not used in this case, the structural integrity was maintained, thus rendering an excellent strengthening and stiffening effect in the sample. To further determine the deformation and failure mechanism of the bulk nanolaminated nanocarbon-metal composite, graphene (in the form of reduced graphene oxide, RGO)-aluminum micro-pillars of various laminate

orientations were fabricated (Fig. 4a) [18]. The “90° pillar” corresponds to the iso-stress configuration, under which the RGO reinforcement layers do not share mechanical load upon deformation. The iso-strain (“0°”) pillar bears the load during uniaxial compression, while the micro-pillar with 45°-slanted RGO/Al interfaces has the maximum resolved shear stress at the interfaces during deformation (“45° pillars”), so that the interfacial shear strength of the composite can be evaluated. For comparison, 0° and 90° pure aluminum pillars fabricated using the same processing parameters are produced. Compressive true stress vs. true strain curves shown in Fig. 4b indicate that the 0° and 90° pure aluminum pillars have similar strengths (216 ± 15 MPa vs. 209 ± 28 MPa, respectively), while the composite micro-pillars display significant property anisotropy, i.e., the 0° pillars have the highest strength of 513 ± 69 MPa, the 45° pillars the lowest strength of 267 ± 68 MPa, and the 90° pillars have an intermediate strength of 322 ± 27 MPa. The iso-strain 0° composite pillars therefore exhibit a clear load-sharing effect, and the iso-stress 90° pillars are still much stronger than their pure aluminum counterpart, which can be attributed to the enhanced dislocation pile-up resulting from the graphene

layers incorporated at the inter-lamella interfaces [37,42]. Post-deformation TEM analysis further clarifies the failure mechanism of the composite pillars of different orientations (Fig. 5). In particular, the “shear angle” (the angle between the shear fracture plane and the pillar cross-section) in the 0° composite pillars is on the order of 20–30°, but it becomes 50–60° for the 90° composite pillars. This suggests that the graphene/aluminum interfaces tend to deviate the fracture path towards the orientation which parallels the interfaces, showing an appreciable crack deflection mechanism. However, in the case of 45° composite pillars, no such toughening mechanism is at work, thus quick crack propagation develops after its initiation (presumably at the voids near the interfaces with insufficient densifications) at the lowest strength.

4. Perspectives and challenges

This article reviews recent developments in measuring the interfacial properties in advanced MMCs, with an emphasis on the use of micro-/ nano-mechanical testing approaches. It is shown that, with novel in situ conditions, including cyclic [43], high temperature [44,45] and

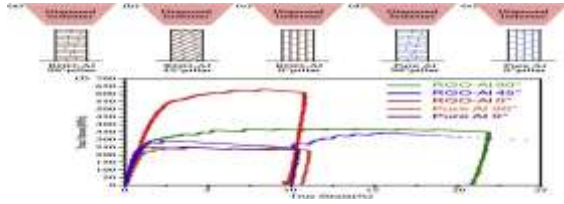


Fig. 4. Schematic of compression tests of $\sim 1.5 \mu\text{m}$ -diameter 1.50 vol % RGO-Al composite pillars and Pure Al pillars with different laminate orientations [18]. Samples are denoted by the angles formed between the laminates and the pillar axis: (a) RGO-Al 90_ composite, (b) RGO-Al 45_ composite, (c) RGO-Al 0_ composite, (d) Pure Al 90_ and (e) Pure Al 0_ pillars, and (f) compressive true stress vs. true strain responses (reprinted with permission from Ref. [18]).

Q. Guo et al. Nano Materials Science 2 (2020) 66–7169. irradiation[46,47]. This constitutes a promising and emerging research direction. However, because both mechanical strength and flow behavior may show notable size effects when the dimension of the material is reduced to small scales [31,48], caution should be used when micro-/ nano-mechanical techniques are employed to explain the deformation mechanisms of bulk materials with “real” structures. This is particularly true for bulk MMC test specimens in which both external and internal microstructural length scales

would be present. Thus, to correctly extrapolate bulk behavior from the micro-/nano-mechanical test results and gain insights into the deformation mechanisms of real, engineering

MMCs, the careful design of specimen dimensions is required, so that the micro-/nano-scale sample is large enough to properly reflect macroscopic materials' properties but is still small enough to be processed using a reasonable timeframe and experimental effort.

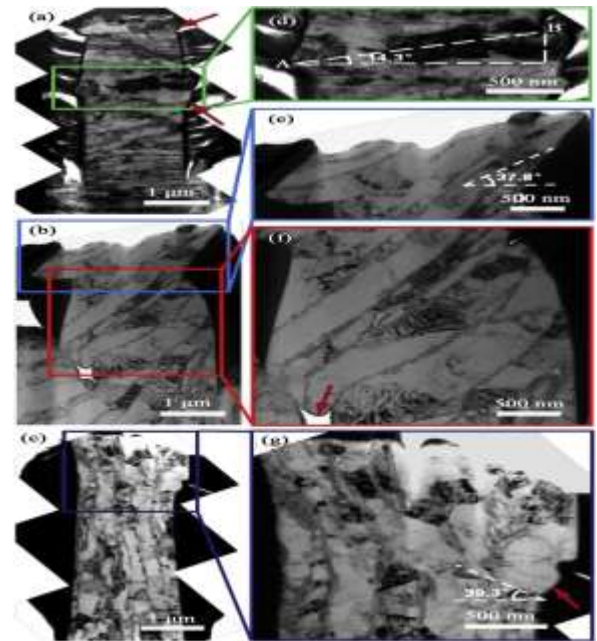


Fig. 5. TEM montages of post-compression 1.50 vol % RGO-Al pillars with different RGO orientations (90_ , 45_ and 0_) [18]. (a)–(c) TEM montages of the entire RGO-Al

90°, 45° and 0° composite pillars, respectively; (d)–(g) magnified renditions of the boxed regions in (a)–(c). The shear angle (the angle between the shear fracture plane and the pillar cross-section) estimate was illustrated in (d), (e) and (g), where the ends of the sheared part aided the identification of the crack propagation path (Point A and Point B in d) (reprinted with permission from Ref. [18]).

Acknowledgements

This work was supported by financial support from the National Key Research and Development Program of China (No. 2017YFB0703103, 2016YFE0130200), the Natural Science Foundation of China (Nos. 51771111), and the Science & Technology Committee of Shanghai Municipality (No. 17520712400).

References

[1] A.C. Collop, Deformation and Fracture Mechanics of Engineering Materials, in: W. Richard (Ed.), fourth ed., Hertzberg John Wiley, Chichester, UK, 1996, ISBN 0- 471-01214-9, p. 786, [https://doi.org/10.1016/S0141-0296\(97\)81125-X](https://doi.org/10.1016/S0141-0296(97)81125-X). £24.95.

[2] L. Jiang, H.M. Wen, H.R. Yang, T. Hu, T. Topping, D.L. Zhang,

E.J.Lavernia, J.M.Schoenung, Influence of length-scales on spatial distribution and interfacial

characteristics of B4C in a nanostructured Al matrix, *Acta Mater.* 89 (2015)327–343, <https://doi.org/10.1016/j.actamat.2015.01.062>.

[3] Y. Wu, G.-Y. Kim, I.E. Anderson, T.A. Lograsso, Fabrication of Al6061 composite with high SiC particle loading by semi-solid powder processing, *Acta Mater.* 58 (13)(2010) 4398–4405, <https://doi.org/10.1016/j.actamat.2010.04.036>.

[4] Y. Zhang, X. Li, Bioinspired, graphene/Al₂O₃ doubly reinforced aluminum composites with high strength and toughness, *Nano Lett.* 17 (11) (2017)6907–6915, <https://doi.org/10.1021/acs.nanolett.7b03308>.

[5] J.D. Currey, Mechanical properties of mother of pearl in tension, *Proc.soc.lond.b196* (1125) (1977) 443–463, <https://doi.org/10.1098/rspb.1977.0050>.

[6] J.D. Currey, Materials science. Hierarchies in biomineral structures, *Science* 309(5732) (2005) 253–254, <https://doi.org/10.1126/science.1113954>.

[7] A.P. Jackson, J.F.V. Vincent, D. Briggs, R.A. Crick, S.F. Davies, M.J. Hearn, R.M.

Turner, Application of surface analytical techniques to the study of fracture surfaces of mother-of-pearl, *J. Mater. Sci. Lett.* 5(10) 975-978,

<https://doi.org/10.1007/bf01730253>.

[8] M. Vedani, E. Gariboldi, Damage and ductility of particulate and short-fibre AlAl₂O₃ composites, *Acta Mater.* 44 (8) (1996) 3077–3088,

[https://doi.org/10.1016/1359-](https://doi.org/10.1016/1359-6454(95)004378)

[6454\(95\)004378](https://doi.org/10.1016/1359-6454(95)004378).

[9] L.J. Bonderer, A.R. Studart, L.J. Gauckler, Bioinspired design and assembly of platelet reinforced polymer films, *Science* 319 (5866) (2008) 1069–1073, <https://doi.org/10.1126/science.1148726>.

[10] L. Zhao, Q. Guo, Z. Li, D.-B. Xiong, S. Osovski, Y. Su, D. Zhang, Strengthening and

deformation mechanisms in nanolaminated graphene-Al composite micro-pillars affected by graphene in-plane sizes, *Int. J. Plast.* 116 (2019) 265–279, <https://doi.org/10.1016/j.ijplas.2019.01.006>.

doi.org/10.1016/j.ijplas.2019.01.006.

[11] H. Gao, B. Ji, I.L. Jager, E. Arzt, P. Fratzl, Materials become insensitive to flaws at

nanoscale: lessons from nature, *P Natl Acad Sci USA* 100 (10) (2003) 5597–5600,

<https://doi.org/10.1073/pnas.0631609100>.

[12] L. Jiang, H. Yang, J.K. Yee, X. Mo, T. Topping, E.J. Lavernia, J.M. Schoenung, Toughening of aluminum matrix nanocomposites via spatial arrays of boron carbide spherical nanoparticles, *Acta Mater.* 103 (2016) 128–140, <https://doi.org/10.1016/j.actamat.2015.09.057>.

[13] Y. Kim, J. Lee, M.S. Yeom, J.W. Shin, H. Kim, Y. Cui, J.W. Kysar, J. Hone, Y. Jung,

S. Jeon, S.M. Han, Strengthening effect of single-atomic-layer graphene in metal graphene

nanolayered composites, *Nat. Commun.* 4 (2013) 2114, <https://doi.org/10.1038/ncomms3114>.

[14] O. Renk, V. Maier-Kiener, I. Issa, J.H. Li, D. Kiener, R. Pippan, Anneal hardening and elevated temperature strain rate

sensitivity of nanostructured metals: their relation to intergranular dislocation accommodation, *Acta Mater.* 165 (2019) 409–419,

<https://doi.org/10.1016/j.actamat.2018.12.002>.

[15] Z.H. Cao, Y.P. Cai, C. Sun, Y.J. Ma, M.Z. Wei, Q. Li, H.M. Lu, H. Wang, X. Zhang,

X.K. Meng, Tailoring strength and plasticity of Ag/Nb nanolaminates via intrinsic

- microstructure and extrinsic dimension, *Int. J. Plast.* 113 (2019) 145–157, <https://doi.org/10.1016/j.ijplas.2018.09.012>.
- [16] Z. Li, Q. Guo, Z. Li, G. Fan, D.B. Xiong, Y. Su, J. Zhang, D. Zhang, Enhanced mechanical properties of graphene (reduced graphene oxide)/aluminum composites with a bioinspired nanolaminated structure, *Nano Lett.* 15 (12) (2015) 8077–8083, <https://doi.org/10.1021/acs.nanolett.5b03492>.
- [17] Z. Li, H. Wang, Q. Guo, Z. Li, D.B. Xiong, Y. Su, H. Gao, X. Li, D. Zhang, Regain strain-hardening in high-strength metals by nanofiller incorporation at grain boundaries, *Nano Lett.* 18 (10) (2018) 6255–6264, <https://doi.org/10.1021/acs.nanolett.8b02375>.
- [18] S. Feng, Q. Guo, Z. Li, G. Fan, Z. Li, D.-B. Xiong, Y. Su, Z. Tan, J. Zhang, D. Zhang, Strengthening and toughening mechanisms in graphene-Al nanolaminated composite micro-pillars, *Acta Mater.* 125 (2017) 98–108, <https://doi.org/10.1016/j.actamat.2016.11.043>.
- [19] X.W. Gu, C.N. Loynachan, Z. Wu, Y.-W. Zhang, D.J. Srolovitz, J.R. Greer, Size-Dependent deformation of nanocrystalline Pt nanopillars, *Nano Lett.* 12 (12) (2012) 6385–6392, <https://doi.org/10.1021/nl3036993>.
- [20] K.S. Ng, A.H.W. Ngan, Deformation of micron-sized aluminium bi-crystal pillars, *Phil. Mag.* 89 (33) (2009) 3013–3026, <https://doi.org/10.1080/14786430903164614>.
- [21] A. Kunz, S. Pathak, J.R. Greer, Size effects in Al nanopillars: single crystalline vs. bicrystalline, *Acta Mater.* 59 (11) (2011) 4416–4424, <https://doi.org/10.1016/j.actamat.2011.03.065>.
- [22] Z.H. Aitken, D. Jang, C.R. Weinberger, J.R. Greer, Grain boundary sliding in aluminum nano-Bi-crystals deformed at room temperature, *Small* 10 (1) (2014) 100–108, <https://doi.org/10.1002/sml.201301060>.
- [23] D. Jang, J.R. Greer, Size-induced weakening and grain boundary-assisted deformation in 60 nm grained Ni nanopillars, *Scripta Mater.* 64 (2011) 77–80, <https://doi.org/10.1016/j.scriptamat.2010.09.010>.
- [24] X.W. Gu, Z. Wu, Y.-W. Zhang, D.J. Srolovitz, J.R. Greer, Microstructure versus flaw:

mechanisms of failure and strength in nanostructures, *Nano Lett.* 13 (2011)

5703–5709,

<https://doi.org/10.1021/nl403453h>.

[25] D.R.P. Singh, N. Chawla, G. Tang, Y.-L. Shen, Micropillar compression of Al/SiC nanolaminates, *Acta Mater.* 58 (2010) 6628–6636.

[26] S. Lotfian, M. Rodríguez, K.E. Yazdanie, N. Chawla, J. Llorca, J.M. Molina-Aldareguía,

High temperature micropillar compression of Al/SiC nanolaminates, *Acta Mater.* 61

(2012) 4439–4451,

<https://doi.org/10.1016/j.actamat.2010.08.025>.

[27] X. Guo, Q. Guo, Z. Li, G. Fan, D.-B. Xiong, Y. Su, J. Zhang, C.L. Gan, D. Zhang, Interfacial strength and deformation mechanism of SiC–Al composite micropillars,

Scripta Mater. 114 (2016) 56–59,

<https://doi.org/10.1016/j.scriptamat.2015.11.018>.

[28] Y.S. Suh, S.P. Joshi, K.T. Ramesh, An enhanced continuum model for sizedependent

strengthening and failure of particle-reinforced composites, *Acta Mater.*

57 (2009) 5848–5861,

<https://doi.org/10.1016/j.actamat.2009.08.010>.

[29] J.C. Shao, B.L. Xiao, Q.Z. Wang, Z.Y. Ma, K. Yang, An enhanced FEM model for particle size dependent flow strengthening and interface damage in particle

reinforced metal matrix composites, *Compos. Sci. Technol.* 71 (2011) 39–45, <https://doi.org/10.1016/j.compscitech.2010.09.014>.

[30] R. Gu, A.H.W. Ngan, Effects of pre-straining and coating on plastic deformation of

aluminum micropillars, *Acta Mater.* 60 (2012) 6102–6111, <https://doi.org/10.1016/j.actamat.2012.07.048>.

[31] J.R. Greer, J.T.M.D. Hosson, Plasticity in small-sized metallic systems: intrinsic versus extrinsic size effect, *Prog. Mater. Sci.* 56 (6) (2011) 654–724, <https://doi.org/10.1016/j.pmatsci.2011.01.005>.

[32] S. Chin Tjong, Recent progress in the development and properties of novel metal matrix nanocomposites reinforced with carbon nanotubes and graphene nanosheets, *Mater. Sci. Eng. R Rep.* 74 (10) (2013) 281–350, <https://doi.org/10.1016/j.mser.2013.08.001>.

[33] A. Nieto, A. Bisht, D. Lahiri, C. Zhang, A. Agarwal, Graphene reinforced metal and

ceramic matrix composites: a review, *Metall. Rev.* 62 (5) (2016) 241–302, <https://doi.org/10.1080/09506608.2016.1219481>.

[34] M.M. Khan, A. Nemati, Z.U. Rahman, U.H. Shah, H. Asgar, W. Haider, Recent advancements in bulk metallic glasses and their applications: a review, *Crit. Rev. Solid State Mater. Sci.* 1–36 (2018), <https://doi.org/10.1080/10408436.2017.1358149>.

[35] C. Lee, X. Wei, J.W. Kysar, J. Hone, Measurement of the elastic properties and intrinsic strength of monolayer Graphene, 321, 2008, pp. 385–388, <https://doi.org/10.1126/science.1157996>, 5887.

[36] Y. Kim, J. Lee, M.S. Yeom, J.W. Shin, H. Kim, Y. Cui, J.W. Kysar, J. Hone, Y. Jung, S. Jeon, Strengthening effect of single-atomic-layer graphene in metal–graphene nanolayered composites, *Nat. Commun.* 4 (2013) 2114, <https://doi.org/10.1038/ncomms3114>.

[37] L. Zhao, Q. Guo, Z. Li, Z. Li, G. Fan, D.-B. Xiong, Y. Su, J. Zhang, Z. Tan, D. Zhang, Strain-rate dependent deformation mechanism of graphene-Al nanolaminated composites studied using micro-pillar compression, *Int. J. Plast.* 105 (2018)

128–140,

<https://doi.org/10.1016/j.ijplas.2018.02.006>.

[38] B. Chen, J. Shen, X. Ye, L. Jia, S. Li, J. Umeda, M. Takahashi, K. Kondoh, Length effect of carbon nanotubes on the strengthening mechanisms in metal matrix composites, *Acta Mater.* 140 (2017) 317–325, <https://doi.org/10.1016/j.actamat.2017.08.048>.

[39] D.L. Zhang, Processing of advanced materials using high-energy mechanical milling, *Prog. Mater. Sci.* 49 (3–4) (2004) 537–560, [https://doi.org/10.1016/S0079-6425\(03\)00034-3](https://doi.org/10.1016/S0079-6425(03)00034-3).

[40] D.B. Witkin, E.J. Lavernia, Synthesis and mechanical behavior of nanostructured materials via cryomilling, *Prog. Mater. Sci.* 51 (1) (2006) 1–60, <https://doi.org/10.1016/j.pmatsci.2005.04.004>.

[41] Z. Li, G. Fan, Q. Guo, Z. Li, Y. Su, D. Zhang, Synergistic strengthening effect of graphene-carbon nanotube hybrid structure in aluminum matrix composites, *Carbon* 95 (2015) 419–427, <https://doi.org/10.1016/j.carbon.2015.08.014>.

[42] Z. Li, L. Zhao, Q. Guo, Z. Li, G. Fan, C. Guo, D. Zhang, Enhanced dislocation obstruction in nanolaminated graphene/Cu composite as revealed by stress

relaxation experiments, *Scripta Mater.* 131 (2017) 67–71, <https://doi.org/10.1016/j.scriptamat.2017.01.015>.

[43] Y. Kim, J. Baek, S. Kim, S. Kim, S. Ryu, S. Jeon, S.M. Han, Radiation resistant vanadium-graphene nanolayered composite, *Sci. Rep.* 6 (2016) 24785, <https://doi.org/10.1038/srep24785>.

[44] J.M. Wheeler, C. Niederberger, C. Tessarek, S. Christiansen, J. Michler, Extraction of plasticity parameters of GaN with high temperature, in situ micro-compression, *Int. J. Plast.* 40 (2013) 140–151, <https://doi.org/10.1016/j.ijplas.2012.08.001>.

[45] R. Soler, J.M. Wheeler, H.-J. Chang, J. Segurado, J. Michler, J. Llorca, J.M. Molina-Aldareguia, Understanding size effects on the strength of single crystals through high-temperature micropillar compression, *Acta Mater.* 81 (2014) 50–57, <https://doi.org/10.1016/j.actamat.2014.08.007>.

[46] J.D.C. Teixeira, D.G. Cram, L. Bourgeois, T.J. Bastow, A.J. Hill, C.R. Hutchinson, On the strengthening response of aluminum alloys containing shear-resistant plateshaped precipitates, *Acta Mater.* 56 (2008) 6109–6122, <https://doi.org/10.1016/j.actamat.2008.08.023>.

[47] K.P. So, D. Chen, A. Kushima, M. Li, S. Kim, Y. Yang, Z. Wang, J.G. Park, Y.H. Lee,

R.I. Gonzalez, Dispersion of carbon nanotubes in aluminum improves radiation resistance, *Nano. Energy* 22 (2016) 319–327, <https://doi.org/10.1016/j.nanoen.2016.01.019>.

[48] S.S. Brenner, Tensile strength of whiskers, *J. Appl. Phys.* 27 (2012) 1484, <https://doi.org/10.1063/1.1722294>.

Q. Guo et al. *Nano Materials Science* 2 (2020) 66–71
71